PULSED H⁻ BEAMS FROM PENNING SPS SOURCES EQUIPPED WITH CIRCULAR EMITTERS

H. Vernon Smith, Jr., Joseph D. Sherman, and Paul Allison
MS-H818, Los Alamos National Laboratory, Los Alamos NM 87545

Abstract

We report the H⁻ beam currents and emittances produced when Penning Surface-Plasma Sources (SPS), equipped with circular emitters, are pulsed at ~1% duty factor. Two sources are now under investigation: the small-angle source (SAS) and the 4X source. The 4X source is designed to test the plasma scaling laws for Penning SPS; SAS is the 1X device. The 0.16 cm³ discharge volume of the SAS is ~30 times smaller than that of the 4X source, 4.6 cm³. With a 0.25-cm-diam circular emitter, the SAS produces 82 mA of 27-keV H⁻ beam with normalized rms emittance of 0.0053×0.0056 $(n \cdot cm \cdot mrad)^2$. With a 0.26-cm-diam circular emitter, the 4X source produces 50 mA of 29-keV H⁻ beam with emittance of 0.0049×0.0050 $(n \cdot cm \cdot mrad)^2$. The measured data are compared with the predictions of the ion-optical code SNOW.

Introduction

Surface-Plasma Sources (SPS) are now being used in pulsed H⁻ injectors on several different accelerators, including those at Brookhaven National Laboratory[1], Fermilab[2], Los Alamos National Laboratory[3], and the Rutherford Laboratory[4]. SPS are typically used with slit emitters, although some work on circular emitters has been reported.[1,5] We began the present study of Penning SPS equipped with circular emitters because of the prospect of simplified beam transport to an accelerator. The H⁻ currents and emittances that can be achieved are of particular interest to us.

SAS Experimental Results

The SAS evolved from Dudnikov's original design[6] and the subsequent Novosibirsk modification[7] of that design. It typically operates at ~0.5% duty factor and produces ~150 mA of pulsed H⁻ beam with rms normalized emittance of 0.006×0.017 $(n \cdot cm \cdot mrad)^2$ from a 0.08×0.7 cm² slit emitter. The beam fraction is typically 40% for the rms emittance and 86% for the 4rms emittance. The emission current density j_{H^-} is 2.7 A/cm². With a 0.25-cm-diam circular emitter, a 0.30-cm-diam extractor, and a 0.26 cm gap, the SAS produces 82 mA of pulsed 27-keV H⁻ beam with 0.0053×0.0056 $(n \cdot cm \cdot mrad)^2$ emittance (Table I). The emission current density is 1.7 A/cm², about 60% of the slit beam result. Figure 1 shows a sample H⁻ beam-
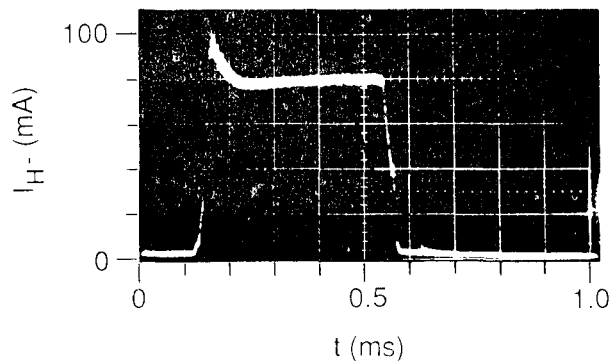
Fig. 1. Oscillogram for a 27-keV, 80-mA pulsed H⁻ beam from a 0.25-cm-diam emitter on the SAS. The bandwidth on the H⁻ current pulse is 1 MHz.

TABLE I. COMPARISON OF THE SAS AND 4X SOURCES

	SAS	4X Source
Cathode-cathode gap, mm	4.3	17
Discharge slot width, mm	3	17
Discharge slot length, mm	12	16
Discharge magnetic field, T	0.22	0.04
Emitter diameter (2R), mm	2.5	2.6
Extraction gap, mm	2.6	3.0
Extraction voltage, kV	27	29
Discharge voltage, V	100	92
Discharge current, A	120	180
Maximum H⁻ current, mA	100 [a]	80 [a]
Maximum j_{H^-}, A/cm²	2.0	1.5
Maximum $j_{H^-}R$, A/cm	0.25	0.20
Gas flow, T ℓ/s	1.3 [b]	0.63
Discharge pulse length, ms	1	2
Repetition rate, Hz	5	5
I_{H^-} for emittance measurement, mA	82	50
H⁻ beam noise, % (peak to peak)	±3	±5
e⁻ current, mA	220	150
Effective kT_x, eV	6.8 [c]	5.3 [c]
ε_x, $n \cdot cm \cdot mrad$	0.0053	0.0049
ε_y, $n \cdot cm \cdot mrad$	0.0056	0.0050

a) Discharge parameters given are for the H⁻ current at which the emittance was measured, not the maximum H⁻ current.

b) This estimate of the H_2 gas flow during the discharge is obtained by dividing the measured average gas flow, 0.063 T ℓ/s, by the gas pulse duty factor, 5%.

c) Calculated from $kT_x = 4 \varepsilon_x^2 mc^2 / R^2$, where mc^2 is the H⁻ mass in eV.

current oscillogram. Figure 2 shows the H⁻ current vs extraction voltage for a discharge current, I_d, of 124A. The H⁻ current is measured in a magnetically and electrically suppressed Faraday cup. There is no indication that the H⁻ current has saturated, even at the highest extraction voltage, although 30 kV is the limit of stable high-voltage operation. For the data in Fig. 2, the H⁻ current has an exponential dependence on extraction voltage to the 2.4 power. The x-plane emittance vs the extraction voltage for $I_d = 120$ A is given in Fig. 3. The y-plane emittance shows similar behavior.
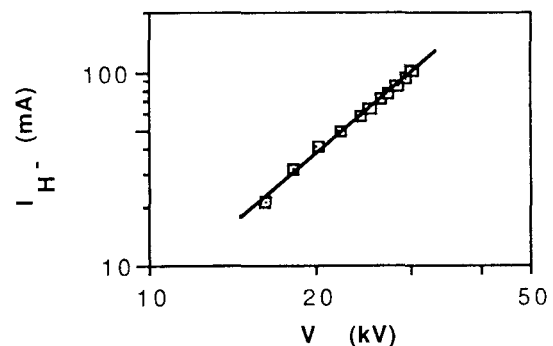
Fig. 2. The extracted H⁻ current, I_{H^-}, vs the extraction voltage, V, for a 124-A discharge in the SAS. The line is a guide to the eye.
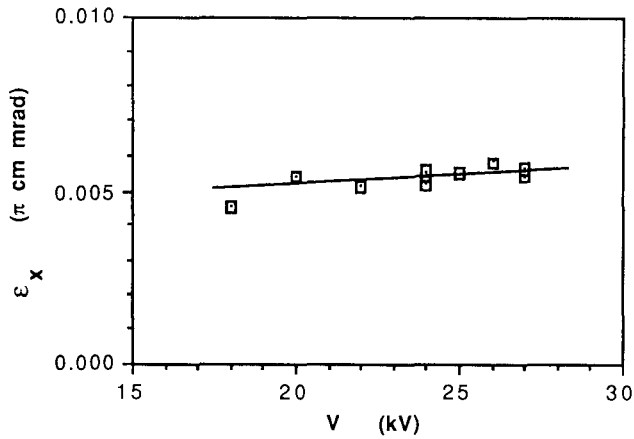
Fig. 3. ε_x vs V for the SAS. These measurements are for I_d held constant at 120A. The line is a guide to the eye.

4X Source Experimental Results

The 4X source is a four times scale-up of the SAS in two of the three spatial dimensions — parallel to the B-field (y) and along the H⁻ beam direction (z), but only a 1.3 times increase in the x-direction.[8] Initial operation of the 4X source with circular emitters was disappointing, with large H⁻ beam fluctuations and beam emittances.[9] We then increased the discharge slot depth (z-direction) to 1.7 cm, which allows operation at low magnetic field (about 500 G) with a resultant drop in the H⁻ beam current fluctuations and H⁻ beam emittance. With a 0.28 x 1.14 cm² rectangular slit, 4X produces 250 mA of 29-keV, pulsed H⁻ beam with emittance 0.014 x 0.027 $(n \cdot cm \cdot mrad)^2$. With a 0.54-cm-diam emitter, it produces 170 mA of pulsed H⁻ beam, and for 150 mA at 23 keV, the emittance is 0.020 x 0.019 $(n \cdot cm \cdot mrad)^2$ with H⁻ beam-current fluctuations of ±1.3%. When the emitter diameter is reduced to 0.26 cm, the maximum pulsed H⁻ beam current decreases to 80 mA. For 50 mA of pulsed 29-keV H⁻ beam, the emittance is 0.0049 x 0.0050 $(n \cdot cm \cdot mrad)^2$ (Table I). The emittance results given here are obtained with the addition of ~1 x 10^{+12}/cm³ of Xe neutralizing gas to the vacuum box.[3] A plot of the x-plane rms normalized emittance vs the extraction voltage is given in Fig. 4 for the 0.26-cm-diam emitter for several different discharge currents. The y-plane emittance shows similar behavior.

The rms emittance has a weak dependence on the H⁻ beam-current fluctuations for the 4X source (Fig. 5), about 1.7% emittance growth per ±1% H⁻ beam fluctuations. This effect is small, but important if the lowest achieveable beam emittance is to be attained. The fluctuations are typically broadband, extending into the megahertz range and can be reduced from as high as ~±50% to ±5% or lower
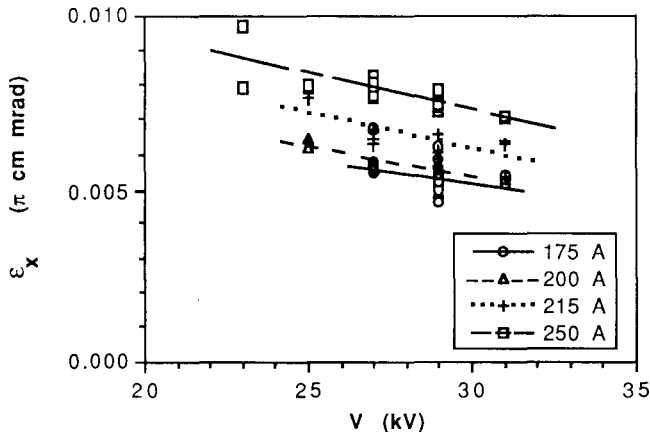
Fig. 4. ε_x vs V for the 4X source for four different arc currents (inset). The lines through the data are guides to the eye.
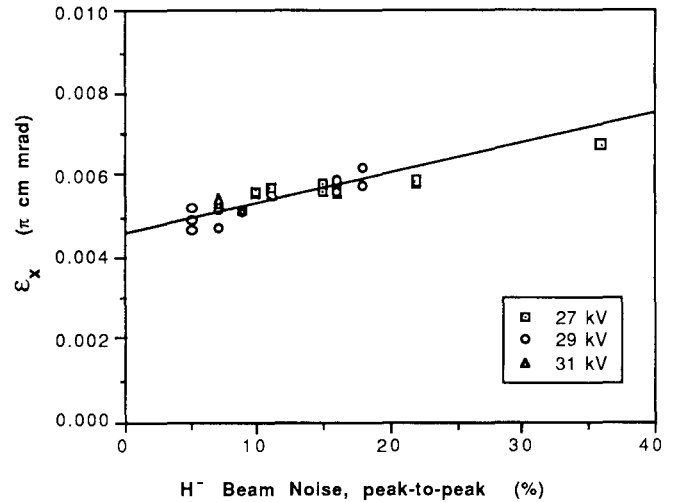
Fig. 5. The rms emittance, ε_x, vs the H⁻ beam noise at three different extraction voltages (inset) for the 4X source. The line through the data is primarily a guide to the eye, but it implies a 1.7% increase in emittance for each ±1% of beam noise. Thus, operation at the lowest noise is desirable, and can be achieved as described in the text.

by proper adjustment of the source H_2 gas flow, Cs flow from an external oven, and magnetic field. The beam fluctuations also influence the rms beam sizes and divergence angles measured at the emittance scanners 12.3 cm downstream from the emitter; the lower the fluctuations, the smaller the spatial and divergence angle sizes of the beam. Minimizing size and divergence angle can be important to the design of a beam-optics system for subsequent transport of the beam to an accelerator.

Ion-Optical Calculations

A sample SNOW[10] simulation with zero ion temperature input for the SAS circular extraction system is shown in Fig. 6a for 81-mA target current at 26 kV. The rms emittance predicted by SNOW for 100% of the beam is 0.0057 $n \cdot cm \cdot mrad$, which includes the emittance contribution from ion-optical aberrations and non-linear space-charge effects. A sample SNOW simulation for the 4X source circular extraction system is shown in Fig. 6b. The extraction voltage is 24 kV, with 56 mA of target current. The SNOW-predicted emittance is 0.0044 $n \cdot cm \cdot mrad$ for 100% of the beam.

The calculated target current, for fixed injection (proportional to discharge) current, as a function of extraction voltage V, is shown in Fig. 7 for the 4X source. For reasons explained below, the results of these calculations are plotted as electron-equivalent beam perveance vs discharge perveance. Neglecting the influence of electron and ion temperatures, SNOW's predictions of beam size, divergence angle, lab emittance, and beam perveance are uniquely specified by the injection perveance for a given geometry.

Comparison of Measurements with SNOW Calculations

The H⁻ current from the 4X source, for several combinations of extraction voltage and discharge current, is displayed in Fig. 7. The SNOW simulation of the 4X source extraction geometry for several different combinations of injection current and extraction voltage is also shown in Fig. 7. The slope of the SNOW-generated curve has been adjusted to agree with the slope of the measurements at low discharge perveance. This linear portion of the SNOW curve corresponds to all of the beam particles being transmitted through the extraction system. The peak in the SNOW curve corresponds to the maximum
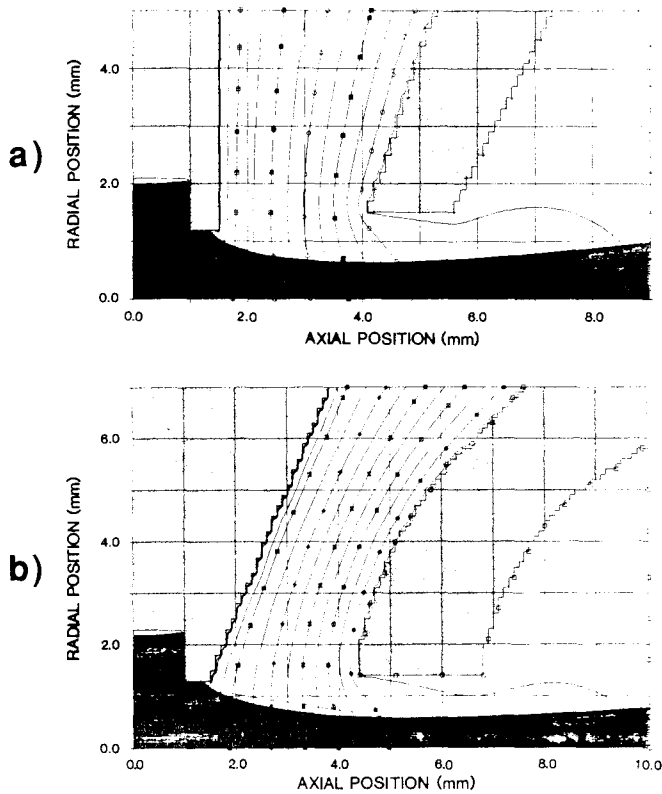
Fig. 6. a) SNOW simulation for the SAS circular extraction system.
b) SNOW simulation for the 4X source circular extraction system.
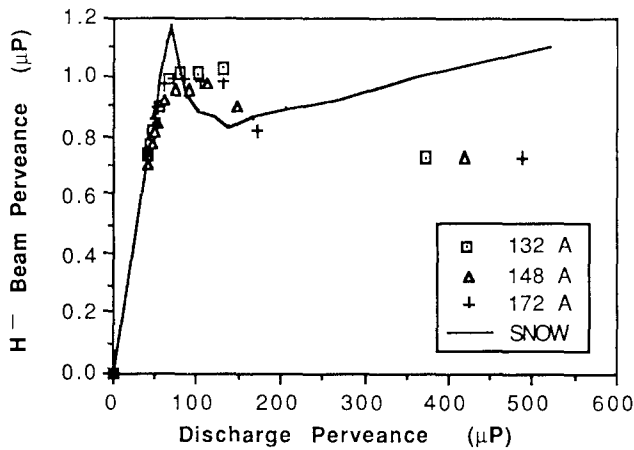
Fig. 7. The measured electron-equivalent H^- beam perveance $[(m_{H^-}/m_e)^{1/2}(I_{H^-}/V^{3/2})]$ vs the discharge perveance $(I_d/V^{3/2})$ for the 4X source. The data are for three different discharge currents (inset). Also plotted on the same graph is the SNOW simulation of the 4X source target perveance vs. the injection perveance.

injection perveance before beam is scraped on the extractor; above this point, scraping occurs.

Neither the magnitudes nor the shapes of the experimental and SNOW curves are in perfect agreement (Fig. 7). Possible reasons for the magnitude difference include (1) neutralization of the H^- ions in the extraction gap; (2) lowered space-charge limit because of the extraction of e^- along with the H^-; (3) possible misalignment of the extraction system, resulting in "lost" H^- beam in the measurements; and (4) either nonuniform or fluctuating emission-current density in the emitter, resulting in "lost" H^- beam on the extraction electrode.

From basic considerations, it would take an e^-/H^- ratio of 7.5/1 to reduce j_{H^-} by 15% from the pure H^- case. Our measured e^-/H^- ratios are typically 1.5-3/1; thus, this effect is about 5%. From the position of the H^- beam in our emittance scanners, we can eliminate (3). Our total H^- beam current has intensity fluctuations (noise) that are typically $< \pm 3\%$. Drifting the measured phase-space diagrams back to the extractor electrode shows that the H^- beam easily fits within the 3-mm-diam extractor hole. Thus, (4) is eliminated as a possible cause of beam loss. This leaves (1) and (2) as the only possibilities. The only species emanating from the source emitter likely to have enough density and an H^- destruction cross section high enough to cause problems are H atoms and H_2 molecules. We calculate H^- destruction by collisions with H atoms and H_2 molecules to be about 20%. The stripping and simultaneous electron extraction effects together are about 25%. Thus, the measured data in Fig. 7 should be corrected upward by 1/0.75 for detailed comparisons with the SNOW curve.

Conclusions

When Penning SPS sources such as the SAS and 4X source are equipped with ~ 0.26-cm-diam circular emitters, transverse rms emittances of about 0.005 n·cm·mrad result. Even though the SAS and the 4X source produce about the same rms transverse emittance, the SAS typically produces about 50% more H^- beam current than the 4X source for the same size emitter. The SNOW simulation code qualitatively predicts the dependence of I_{H^-} on V and I_d. Further work is needed to quantitatively compare this and other ion-beam parameters with the SNOW predictions.

Acknowledgments

References

1. J.G. Alessi, J.M. Brennan, A. Kponou, and K. Prelec, "H⁻ Source and Beam Transport Experiments for a New RFQ," Proc. 1987 Particle Accelerator Conf., IEEE Catalog No. 87CH2387-9, E.R. Lindstrom and L.S. Taylor eds., 304-6 (1987).

2. C.W. Schmidt and C.D. Curtis, "Operation of the Fermilab H⁻ Magnetron Source," AIP Conf. Proc. No. 158, 425-429 (1987).

3. P. Allison and J.D. Sherman, "Operating Experience With a 100-keV, 100-mA H⁻ Injector," AIP Conf. Proc. No. 111, 511-518 (1984).

4. P.E. Gear and R. Sidlow, "Present Status of the Rutherford and Appleton Laboratories' H⁻ Source," Rutherford and Appleton Laboratories report RL-81-050 (July 1981).

5. J.D. Sherman, P. Allison, and H.V. Smith, Jr., "H⁻ Beam Formation from a Penning Surface Plasma Source Using Circular Emission-Extractor Electrodes," Proc. 2nd Int. Symp. on the Prod. and Neutralization of Negative Hydrogen Ions and Beams, Brookhaven National Laboratory report BNL-51304, 184-188 (December, 1980).

6. V.G. Dudnikov, "Surface-Plasma Source of Negative Ions with Penning Geometry," Transactions of the Fourth All-Union Conference on Charged-Particle Accelerators (Nauka Publishers, Moscow, 1975),Vol. 1, p. 323.

7. G.I. Dimov, G. Ye. Derevyankin, and V.G. Dudnikov, "A 100-mA Negative Hydrogen-Ion Source for Accelerators," IEEE Trans. Nucl. Sci. 24 (3), 1545-7 (1977).

8. H.V. Smith, Jr., P. Allison, and J.D. Sherman, "A Scaled, Circular-Emitter Penning SPS for Intense H⁻ Beams," AIP Conf. Proc. No. 111, 458-62 (1984).

9. H.V. Smith, Jr., P. Allison, and J.D. Sherman, "The 4X Source," IEEE Trans. Nucl. Sci. 32, (5) 1797-9 (1985).

10. J.E. Boers, "SNOW—A Digital Computer Program for the Simulation of Ion Beam Devices," Sandia National Laboratory report SAND79-1027 (1980).